Nanoscale

Accepted Manuscript

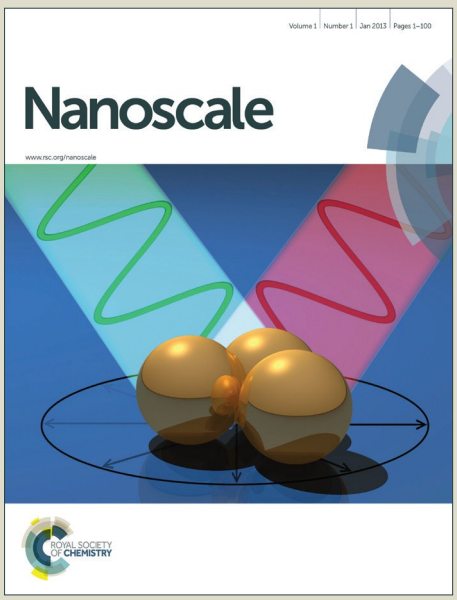

ROYAL SOCIETY OF CHEMISTRY

www.rsc.org/nanoscale

Journal Name

COMMUNICATION

A Novel Cost Effective Fabrication Technique for Highly Preferential Oriented TiO_2 nanotubes.

Received 00th January 20xx,
Accepted 00th January 20xx

DOI: 10.1039/x0xx00000x

www.rsc.org/

Aijo John K[a], Johns Naduvath[b], Sudhanshu Mallick[b], Thoudinja Shripathi[c], Manju Thankamoni[d], and Rachel Reena Philip[a]*

Abstract: Single crystalline like TiO_2 nanotubes with preferential orientation along [001] direction, parallel to the growth direction of nanotubes, that offer ease of charge transport much higher than so far reported, are fabricated using a cost effective two step technique. The success of this method to grow the nanotubes with the anomalous intense [001] preferential orientation is attributed to the Zinc assisted minimization of the (001) surface energy. The single crystalline like TiO_2 nanotubes show superior performance as super capacitor electrodes compared to the normal polycrystalline titanium dioxide nanotubes.

Uninterrupted pathways for electron transport to the back contact are highly recommended for devices like Dye sensitized solar cells (DSSC), super capacitor and photo catalytic applications. This has incited an ever increasing interest in one dimensional nanostructures such as nanorods and nanotubes of ZnO, TiO_2 etc. that provide directional electron path ways in devices.[1-3] One of the most investigated one dimensional nanostructures of the last decade is titanium dioxide nanotube (TONT) because of its exceptional electronic and structural characteristics.[4,5] Compared to nano particulate film, higher carrier transport properties are expected in one dimensional titanium dioxide nanotubes due to the morphologically ordered nature of nanotubes. Contrary to expectations, TONT do not often show significant enhancement in the transport properties due to the random orientation of the grains in the polycrystalline tubes and grain boundary effects.[6-9] The grain boundaries create recombination centers in the form of interface states and potential barriers, which limit the carrier transport between the crystallites.[10] Hence, fabrication of TiO_2 nanotubes with preferential orientation of their grains along the direction of tube growth is highly advantageous.

Researchers have observed that different processing techniques such as anodization and hydrothermal method that are conventionally adopted for growing TONT yield amorphous tubes, which can be converted to anatase crystalline phase by annealing at a temperature above 280^0C and to rutile phase at temperature above 500^0C. [11,12] But even after annealing, the nanotubes turn up to be polycrystalline with random orientation of grains along (101), (200), (004) etc. planes.[13] In such polycrystalline tubes with random orientation of grains, the electrons have to move in zig- zag manner and lose part of their energy due to scattering from crystallite interfaces.

For device applications of one dimensional TiO2 nanorods and nanotubes, orientation in [001] direction, parallel to the growth direction of the tubes is preferred, as it will enhance the charge transport and charge collection efficiency of the tubes.[14-16] But since the (101) faces are energetically more stable, the processing of TONT in [001] direction is reported to be difficult and challenging.[17-19]

A literature survey shows that different researchers have attempted the fabrication of anatase TiO_2 single crystals with maximum percentage exposure of the highly reactive {001} facets[17-19] as well as synthesis of TONT with (001) orientation.[14-16,20-21] Park *et al*[14] *and* Lee *et al*[20] report optmization of water content in the electrolyte during anodisation as a method to fabricate (004) preferentially oriented TONT where as Jung *et al*[15] *and* Seong *et al*[16] have achieved preferential orientation by surface assisted processes using poly vinyl pyrrolidone and tailoring the surface roughness of the titanium substrates respectively. By the aforementioned techniques Lee et al, Seong et al and Park et al have succeeded in fabricating (004) preferentially oriented TONTs with $I_{(004)}/I_{(200)}$ ratios ~ 17.3, 135 and 200 respectively. Pan *et al* reports fabrication of TONT with $I_{(004)}/I_{(101)}$ ratio of 23.2 for tube lengths ~ 15 µm which is increased to 38.3 for tube lengths ~ 38 µm.[21] Moreover, enhanced electron transport properties and improved photo conversion efficiency are reported for these single crystalline like nanotubes when compared to the polycrystalline. [14-16,20,21]

* Corresponding Author- email: reenatara@gmail.com

[a] Department of Physics
Union Christian college, Aluva, Kerala, India
[b] Department Of Metallurgical Engineering and Material Science
Indian Institute of Technology, Mumbai, Maharashtra, India.
[c] Scientist, UGC-DAE Consortium for Scientific Research
Indore, Madhya Pradesh, India
[d] Department of Physics
Sree Sankara College, Kalady, Kerala, India

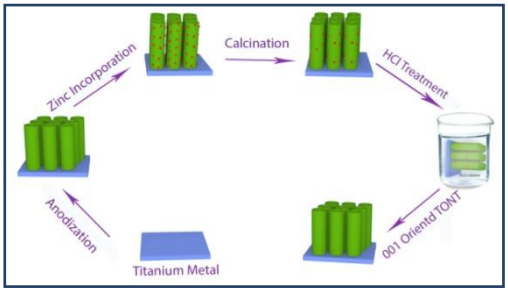

Figure 1. Process flow of the single crystalline like TONT formation

Here, we discuss a novel method to fabricate single crystalline like TiO_2 nanotubes oriented along [001] direction with strikingly higher $I_{(004)}/I_{(101)}$ ratio and hence improved electronic transport than reported so far.[20,21] A schematic diagram of the processing technique of the TONT is given in Fig.1. The tubes are synthesised by a two-stage technique, where in the first stage, well aligned and uniform amorphous TiO_2 nanotubes are fabricated on titanium foil by a cost effective electrochemical anodisation technique. Here for cost reduction, titanium foils are used both as working electrode and counter electrode instead of high-cost platinum counter electrode. The anodization is carried out for two hours at a constant voltage of 50V with 0.5 wt % ammonium fluoride and 2 vol % de-ionized water in ethylene glycol as electrolyte. The surface deposited nanograss is then removed by ultrasonic cleaning in deionised water. The second stage consists of zinc assisted preferential orientation of grains in the nanotubes. In this stage, Zn incorporation in the amorphous nanotubes is done in a three electrode system by applying a negative voltage of 2.5V to titanium dioxide nanotube with 1 M zinc sulphate solution as electrolyte. The zinc incorporated as well as undoped amorphous nanotubes(a-TONT) are annealed in air at 500^0C for 3 hours for the amorphous to crystalline transformation. The surface deposited oxidized zinc on the Zn-incorporated nanotubes (Zn-TONT) is removed by dipping the tubes in 1 M HCl solution for one hour before further characterizations. Zn incorporation has been done for time periods ranging between 1s to 10s keeping all other conditions the same to obtain Zn doping at different concentrations and to optimise the condition for yielding highly preferential oriented single crystalline like nanotubes (s-Zn-TONT).

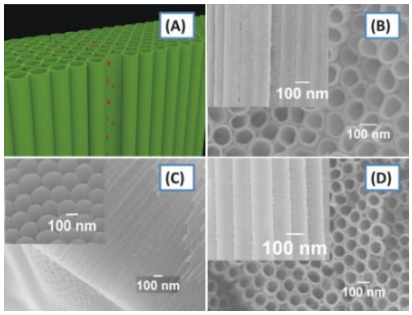

Figure. 2 Schematic and scanning electron microscopy images of the undoped and doped TONTs (A) Schematic of s- Zn-TONT, (B) SEM image top view of p- TONT (B- inset) Tube walls of p- TONT, (C) side view of p- TONT (C-inset) bottom view of p- TONT, (D) top view of s-Zn- TONT(D inset) Tubewalls of s-Zn-TONT.

Morphological characterization by Scanning Electron Microscopy (SEM) using JEOL JSM 7600F Field Emission Scanning Electron Microscope shows that the polycrystalline TONT (p-TONT) obtained after direct annealing of the as-synthesised amorphous TONT (a-TONT) in the first stage have inner diameter of ~ 60 nm and length ~ 15 µm (Fig.2.B, C) with well defined walls and rough grains with clear grain boundaries (Fig.2.B inset). The Zn-incorporated nanotubes after annealing (Fig.2.D) possess smooth tube walls with lesser grain boundaries (Fig.2.D inset).

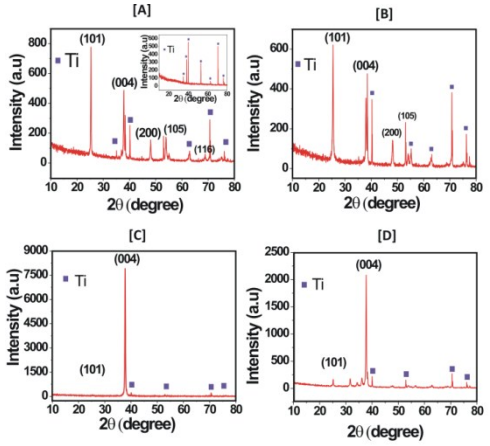

Figure 3. X- ray diffraction images of the Doped and Undoped TONTS (A) p- TONT (A- inset) a-TONT (all the peaks correspond to Ti substrate) (B) Zn-TONT with 3 % Zinc (C) s-Zn-TONT with 6 % Zinc (D) Zn-TONT with 7 % Zinc.

Fig. 3 shows the X- ray diffraction patterns of a-TONT (Fig.3.A inset), p-TONT (Fig.3.A) and Zn-TONTs (Fig.3.B-D) respectively. The diffraction peaks of the p-TONT, correspond to the anatase phase of the nanotubes with orientations along (101), (004), (200), (105) and (116) with preferred orientation along (101). The XRD of Zn-TONTs indicate an enhanced peak intensity ratio $I_{(004)}/I_{(101)}$ compared to that in p- TONT, indicating the tendancy of the grains to orient along (004) plane in the former. Fig.3.C (with 6 % of Zinc doping) shows XRD of a typical TONT with single crystalline like nature (s-Zn-TONT), with strong preferential orientation along the [001] direction ie. (004) plane of anatase phase. In s-Zn-TONT, the texture coefficient of (004) plane is 1997 times greater than that of (101) plane. s-Zn-TONT shows $I_{(004)}/I_{(101)}$ intensity ratio of ~ 77.1, which is 122 times larger than the intensity ratio for a typical p-TONT. On comparing with the standard JCPDS intensity, the observed intensity of the (004) plane is found to be 90 times higher than the standard [JCPDS 89-4203], and comparison with Pan *et al's*[21] nanotubes of comparable tube lengths (15 µm) shows the s-Zn-TONT to possess $I_{(004)}/I_{(101)}$ intensity ratio ~ 3.4 times greater, thus indicating that the novel Zn-assisted method is highly effective in the production of [001] oriented TONTs. A direct comparison of the intensity ratio in the present work can not be made with the reports of Lee et al, Seong et al and Park et al, since their reports pertain to $I_{(004)}/I_{(200)}$ intensity ratio where as no (200) peak is observable here.

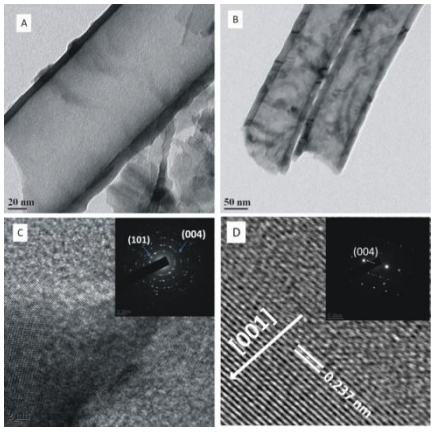

Figure 4. HRTEM images of (A) p- TONT (B) s-Zn-TONT (C) High resolution lattice image of p-TONT-scale 2 nm (C-Inset) SAED image of p- TONT (D)high resolution lattice image of s- Zn- TONT (D-Inset) SAED image of s- Zn- TONT.

High Resolution Transmission Electron Microscopy (HRTEM) images (Fig.4) show well oriented grain structure for s-Zn-TONT (Fig.4D) when compared to that for p-TONT (Fig.4C). The textured (004) planes for s-Zn- TONT are evaluated to have lattice spacing of 0.237 nm. The Selected Area Electron Diffraction (SAED) pattern of s-Zn-TONT(Fig. 4. D inset) shows dot pattern characteristic of single crystalline materials where as p-TONT gives ring pattern (Fig.4.C.inset) indicating different planes characteristic of polycrystalline films.

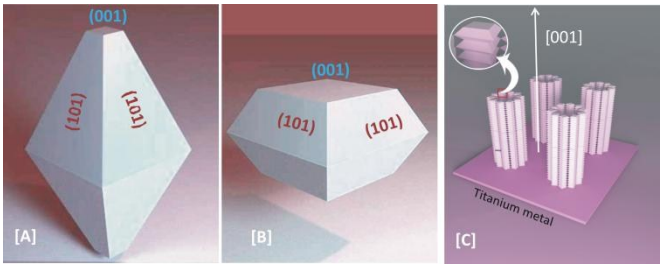

Figure 5. TiO_2 crystallite of **(A)** p-TONT with greater surface area for {101} facet **(B)** s-Zn-TONT with greater surface area for {001} facet **(C)** TiO_2 nanotubes with the greater area {001} facets facing tube top.

To explain the aforementioned highly oriented growth in the [001] direction in s-Zn-TONT, the surface energies of the different facets of TiO_2 and the effect of Zn incorporation is considered. Based on the surface free energy considerations which is a measure of thermodynamic stability of surfaces, it is expected that the {101} facet with lowest surface energy (0.44 J/m^2) has the highest probability of stability in TONT leading to growth of anatase crystals with the larger surface area {101} facets (Fig.5.a) possessing preferential orientation, and hence here the formation of nanotubes with preferential orientation of {001} facets with higher surface energy ~ 0.90 J/m^2 demands assistance by an external agency. [22-24] To fully understand the mechnism behind the anomalous preferential orientation of the Zn- incorporated nanotubes in [001] direction, more characterizations are needed.

However, based on the available data, the mechanism of growth is proposed as follows. When Zn is incorporated into the amorphous tubes and then annealed to trigger crystallisation of the tube {001} facets of the crystallites having high reactivity tend to adsorb Zn ions easily than the other lesser reactive facets. The Zn adsorption on {001} facets reduces the surface energy of the surface, which results in the enhanced surface area of these facets as shown in Fig.5b, till the limit that the differentiate adsorption energy and hence the adsorption ability of the facet becomes weaker than that of the {101} facet, thus impeding further adsorption and growth of {001}.[18] There will be no further reduction in the surface energy of the {001} facet. The crystallites are stacked connecting these facets leading to preferential orientation along [001] direction (fig.5.c), so that the higher area (001) surfaces faces the tube up.[25] Thus here, bonding of Zn ions forming O-Zn bonding with the two fold coordinated oxygen atoms, acts as the external agency that leads to the anomalous intense preferential orientation along the [001] direction.

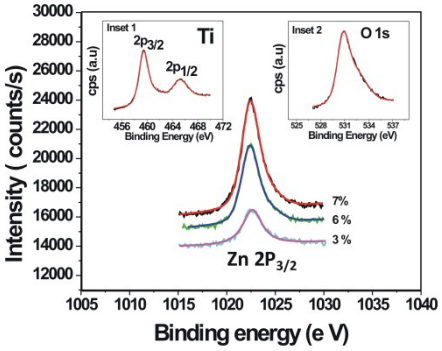

Figure 6. XPS of Zn doped TONTs with different zinc concentration

This explanation agrees with the further analyses using X-ray photoelectron spectroscopy, where the chemical analyses of TONTs prepared under different Zn concentrations have been done assessing the XPS data using VSW Scientific Instruments spectrometer fitted with Mg and Al twin anode X-ray source. The XPS peaks depicting the binding energy positions of Zn, Ti and O in Zn-TONTs corresponding to three different Zinc concentrations are given in Fig. 6. Combining the XPS data in Fig.6 (yielding atomic concentrations of Zn) with the XRD data in Fig.3, it is found that while the $I_{(004)}/I_{(101)}$ ratio from XRD of undoped nanotubes (Fig. 3A) is only 0.63, it is increased to 0.77 (Fig. 3B) for zinc concentration of 3%. As the Zn% is further increased, the (004) preferential orientation increases till at ~ 6% of Zn, the intensity ratio $I_{(004)}/I_{(101)}$ seems to approach an upper limiting value ~ 77.1 (Fig. 3 C). But for doping concentrations higher than this, the ratio is found to reduce, as shown in the case of a 7% Zn doped TONT, where the ratio is decreased to ~ 11.9 (Fig. 3 D). This initial increase in the I_{004}/I_{101} ratio with increase in Zn concentration and the decrease observed when adsorption is extended to longer time period is explained as follows. Zinc ion adsorption on the (001) surface reduces its surface energy for formation till its differential adsorption ability becomes weaker than that of other surfaces. There after, further adsorption is not possible on the (001) surface. More Zn exposure will result in the adsorption of zinc ions on the other surfaces like (101), reducing the surface energy for formation

of these surfaces also and thus resulting in a reduction in $I_{(004)}/I_{(101)}$ intensiy ratio and texture coefficient of (004) plane.

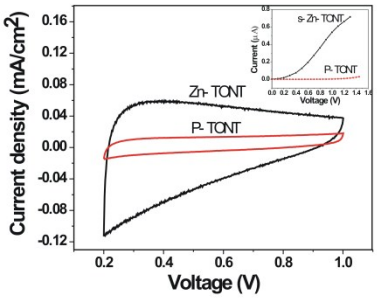

Figure 7. CV curves of p-TONT and s-Zn-TONT (B-inset) I-V characteristics of p- TONT and s-Zn-TONT.

Current–voltage (I-V) characteristics (Fig.7 inset) determined by applying silver electrode on top of the nanotubes show the superior charge transport property of s-Zn-TONT when compared to p-TONT, as expected for these preferentially oriented tubes. The I-V curves are non-linear probably due to a Schottky junction formed at the silver contact and Titanium dioxide nanotube interface. Such schottky junction formation of TiO_2 nanotubes with metal contacts has been earlier observed.[26] The increased conductivity of s-Zn-TONT when compared to p-TONT indicates that the issue of carrier scattering while travelling zig-zag paths in polycrystalline TONT, which has been a limiting factor to the functioning of devices such as DSSC, supercapacitors etc., can be circumvented to a large measure by applying the [001] textured TONT for carrier transport in these devices.

To compare the performance of p-TONT and s-Zn-TONT in supercapacitance applications, the electrochemical characterizations of the nanotubes are done by conducting cyclic voltametry (CV) measurements. The CV data curves obtained by measurement using a three electrode configuration with TONT (p-TONT and s-Zn-TONT) as working electrode and 1 M KCL solution as electrolyte are shown in Fig. 7. The superior performance efficiency, as super capacitor electrodes, of the [001] textured s-Zn-TONT is very clear on comparing its specific capacitance calculated from the integrated area of the CV curves, with that of the p-TONT. The measured specific capacitance of the s-Zn-nanotubes is 380 $\mu F/cm^2$ at scan rate of 300 mV/s, which is 7.2 times higher than that of the p-TONT (53 $\mu F/cm^2$) at the same scan rate. (Fig.7). The experiment affirms that s-Zn-TONTs are excellent candidates for electrode applications in supercapacitors.

Conclusions

A novel cost effective technique where Zn ions aid the fabrication of highly conducting TiO_2 nanotubes with preferential orientation of grains along [001] direction, parallel to the growth direction of the tubes is presented. The structural, morphological and electrical characterizations together with the cyclic voltametry measurements confirm beyond doubt the superior performance abilty of s-Zn-TONT in energy storage devices and their future scope in energy production applications.

Acknowledgements: AJK, MT and RRP acknowledge UGC-DAE, Indore for the funding through a collaborative project and the Saif IIT Bombay for the help with SEM and HRTEM.

References

1 B. Liu, H. C. Zeng, JACS **2003**, 125, 4430.
2 S. H. Lee, T. Minegishi, J. S. Park, S. H. Park, J. S. Ha, H. J. Lee. H. J. Lee, S. Ahn, J. Kim, H. Jean, T. Yao. Nano letters **2008**, 8 2419.
3 B. Liu, E. S. Aydil, JACS **2009**, 131, 3985.
4 J. M. Macak, H. Tsuchiya, A. Ghicov, K. Yasuda, R. Hahn, S. Bauer, P. Schmuki, Current Opinion In Solid State And Materials Science, **2007**, 11, 3.
5 P. Roy, S. Berger, P. Schumuki, angewandte chemie international edition, **2011**, 50, 2904.
6 R. Muhammadpour, A. I. Zad, A. Hagfeldt, G. Boschloo, ChemPhyschem **2010**, 11, 2040.
7 K. D. Benkstien, N. Kopidakis, J. Van de Lagemaat, A. J. Frank J. Phys. Chem. B **2003**, 107, 7759.
8 K. Zhu, T. B Vinzant, N. R. Neale, A. J. Frank, Nano Letters **2007**, 12, 3729
9 P. Docampo, S.Guldin, U. Steiner, H. Snaith, Journal of Physical Chemistry Letters **2013**, 4, 698.
10 J. V. Cab, S. R. Jang, A. F. Halverson, K. Zhu, A. J. Frank, Nano Letters, **2014**, 14, 2305.
11 G. K. Mor, O. K. Varghese, M. Poulose, C. A Grimes, Advanced Functional Materials **2005**, 15, 1291.
12 G. K. Mor, O. K. Varghese, M. Poulose, K. Shankar, C. A Grimes, Sol Energy Mater Sol Cells **2006**, 90, 2011.
13 O. K. Varghese, D. Gong, M. Poulose, K. G. Ong, C. A Grimes E. C. Dickey, Journal of Material Research **2003**, 18, 156.
14 I. J. Park, D. H. Kim, W. M. Seong, B. S. Han, G. S. Han, H. S. Jung, M. Yang, W. Fan, S. Lee, J. K. Lee, K. S. Hong, CrystEngg Comm, **2015,** 17, 7346
15 M. H. Jung, M. J. Chu, M. G. Kang, Chemical Communication, **2012**, 48, 5016.
16 W. M. Seong, D. H. Kim, G. D. Park, K. Kang, S. Lee, K. S. Hong, The Journal of Physical Chemistry C, **2015**, 119, 13297
17 H. G. Yang, C. H. Sun, S. Z. Qiao, J. Zon, G. Lin, S. C. Smith, H. M. Cheng, G. Lu, Nature Letters **2008**, 453, 638.
18 B. Zhang, F. Wai, Q. Wy, L. Piao, M. Liu, Z. Jin, Journal of physical chemistry C, **2015**, 6094.
19 X. Han, D. Kuang, M. Jin, Z. Xie, L.Zheng, JACS, **2009**, 131,3152.
20 S. Lee, I. J.Park, D. H. Kim, W. M. Seong, D.W. Kim, G. S. Han, J. Y. Kim, H. S. Jung, K. S. Hong, Energy Environ. Sci., **2012**, 5, 7989
21 D. Pan, H. Huang, X. Wang, L. Wang, H. Liao, Z. Li, M.Wu, Journal of Material Chemistry A **2014**, 2, 11454.
22 G. Liu, J. C. Ju, G. Q. Lu, H. M. Cheng, Chemical Communication, **2011**, 47, 6763.
23 M. Lazzeri, A. Vittadini, A. Selloni, Physical Review B **2001**, 63, 155409.
24 A. Vittadini, A. Selloni, F. P. Rotzinger, M. Gratzel, Physical Review Letters **1998**, 81, 2954.
25 P. A. Pena, F. Gonzalez, G. Gonzalez, I. Gonzalez, Physical Chemistry Chemical Physics, **2014**, 16, 26213.
26 M. Hattori, K. Noda, T. Nishi, K. Kobayashi, H. Yamada, K. Matsushige, Applied Physics Letters **2013**, 102, 043105.